Stem Cell Reports
Article

OPEN ACCESS

Prostaglandin E_2 Is Required for BMP4-Induced Mesoderm Differentiation of Human Embryonic Stem Cells

Bowen Zhang,[1,2,3] Lijuan He,[1,2,3] Yiming Liu,[1,2] Jing Zhang,[1,2] Quan Zeng,[1,2] Sihan Wang,[1,2] Zeng Fan,[1,2] Fang Fang,[1,2] Lin Chen,[1,2] Yang Lv,[1,2] Jiafei Xi,[1,2] Wen Yue,[1,2] Yanhua Li,[1,2,*] and Xuetao Pei[1,2,*]

[1]Stem Cell and Regenerative Medicine Lab, Beijing Institute of Transfusion Medicine, Beijing 100850, China
[2]South China Research Center for Stem Cell & Regenerative Medicine, SCIB, Guangzhou 510005, China
[3]Co-first author
*Correspondence: shirlylyh@126.com (Y.L.), peixt@nic.bmi.ac.cn (X.P.)
https://doi.org/10.1016/j.stemcr.2018.01.024

SUMMARY

The accurate control of early cell fate specification during differentiation of human embryonic stem cells (hESCs) is critical for acquiring pure therapeutic cell populations of interest. Bone morphogenetic protein 4 (BMP4) is a key mesoderm inducer from ESCs. However, the molecular mechanism of the mesodermal cell fate decision induced by BMP4 remains unclear. Here, we demonstrate the requirement of a bioactive lipid, prostaglandin E_2 (PGE_2), for the mesoderm specification from hESCs by BMP4 induction. We show that BMP4 directly regulates the expression of the key enzyme for PGE_2 synthesis, *COX-1*, and promotes PGE_2 production. More importantly, in the absence of BMP4, forced *COX-1* expression or PGE_2 treatment is sufficient to initiate mesoderm specification of hESCs by activation of EP2-PKA signaling and modulation of nuclear translocation of β-catenin. Together, our findings provide insights into the critical role of BMP regulation of PGE_2 synthesis and its downstream signaling in initiating mesoderm commitment of hESCs.

INTRODUCTION

Human embryonic stem cells (hESCs) derived from the inner cell mass have a capacity for long-term self-renewal and can differentiate into cells of all three germ layers (Thomson et al., 1998). Among the three embryonic germ layers, the mesoderm lineage gives rise to diverse tissues including blood, heart, and muscle. This unique property makes hESCs an attractive tool for various cell-based therapeutic applications and disease modeling (Murry and Keller, 2008). Although the development of mesoderm tissues is well studied and characterized *in vivo* and *in vitro* at embryo and cellular levels, the molecular mechanism of this process remains poorly understood. Previous studies have suggested that bone morphogenetic protein (BMP) is a critical gastrulation regulator that induces the primitive streak and mesoderm formation in embryos (Beppu et al., 2000; Mishina et al., 1995; Winnier et al., 1995). Short-term BMP4 treatment can mediate the induction of primitive streak and mesoderm lineage differentiation of mouse ESCs and hESCs (Drukker et al., 2012; Ng et al., 2005; Wang et al., 2012; Wiles and Johansson, 1997; Zhang et al., 2008). In addition to BMP4 signaling, canonical Wnt and Activin-Nodal signaling also participate in driving differentiation of pluripotent stem cells toward mesendoderm and mesoderm lineages (Chng et al., 2010; Kurek et al., 2015; Matulka et al., 2013; Singh et al., 2012; ten Berge et al., 2008; Vallier et al., 2009). In recent years, significant advances have been made in understanding the events that control early lineage differentiation through using hESC modeling of the differentiation *in vitro*. However, precise mechanisms by which microenvironmental factors and intracellular molecules promote specific programs of mesendoderm and early mesoderm differentiation remain to be elucidated.

Prostaglandin E_2 (PGE_2) has been known to mediate numerous physiological events, such as reproduction, angiogenesis, hematopoietic stem cell proliferation, and homing (Hoggatt et al., 2009; Leahy et al., 2000; Ruan et al., 2012). Recent studies suggest that PGE_2 is required for early vertebrate embryogenesis, specifically gastrulation, a key process in the formation of the germ layers (Goessling et al., 2009; Speirs et al., 2010). Interference with the expression of cyclooxygenase-1 (COX-1, also known as PTGS1), the key enzyme responsible for the synthesis of PGE_2, results in gastrulation arrest, mainly due to disruption of the stability of Snai1a and excessive cell adhesion (Speirs et al., 2010). Further studies suggest that PGE_2 also participates in mesoderm-derived cell differentiation from ESCs (Yang et al., 2010; North et al., 2007). The key role observed for PGE_2 and its synthesis enzymes in the zebrafish development model and ESC differentiation led us to investigate its function in the early mesoderm specification of human pluripotent stem cells.

Here, we report that PGE_2 signaling plays a critical role in the initiation of the mesoderm differentiation of human pluripotent stem cells. Inhibition of PGE_2 synthesis by indomethacin significantly blocked the BMP4-induced mesoderm differentiation and promoted neuroectoderm commitment of hESCs. COX-1, one of the key enzymes responsible for PGE_2 synthesis, is required for mesoderm specification of hESCs. Its expression is directly

This is an open access article under the CC BY-NC-ND license (http://creativecommons.org/licenses/by-nc-nd/4.0/).

regulated by BMP4 signaling in hESCs. Subsequently, PGE_2 can bypass BMP4 signal and stimulate the mesoderm differentiation of hESCs via the EP2-PKA-GSK3β/β-catenin signaling pathway. Thus, our data provide insights into the function of COX-1-regulated PGE_2 signaling in the initiation of the mesoderm specification of human pluripotent stem cells and suggest that this signaling pathway plays a critical role in early embryo development.

RESULTS

PGE_2 Level Increases upon BMP4-Induced Mesoderm Differentiation

It has been reported that BMP4 signaling is dispensable in the initiation of gastrulation and mesoderm differentiation. We also found that BMP4 was the one of the strongest mesoderm inducers to promote the expression of mesoderm initiation marker genes (*BRACHYURY*, *TBX3*, and *MIXL-1*) and key proteins BRACHYURY (BRA) and MIXL-1 in the process of hESC differentiation (Figures S1A–S1D). By culturing hESCs in a serum-free defined medium (SFDM) with BMP4 for 48 hr (Figure 1A), the morphology of these hESCs changed from round, dense colonies into loose patches with more flattened cells in the surroundings (Figure 1B). qPCR analysis showed significant upregulation of expression of the mesendodermal and early mesodermal marker genes, such as *BRA*, *TBX3*, *MIXL-1*, *EOMESODERMIN* (*EOMES*), *WNT3*, and *PDGFRα*, whereas the expression of a pluripotent and early neuroectodermal gene, *SOX2*, was downregulated after BMP4 induction (Figure 1C). Immunofluorescence staining results indicated that most of the differentiated cells coexpressed BRA, EOMES, and TBX3 upon BMP4 induction (Figure 1D), reflecting mesendoderm and early mesoderm specification. The expression of *OCT4* gene and protein presented little change (Figures 1C and S1E), which is consistent with its role in mesoderm commitment. To identify the potential role of PGE_2 in regulating mesoderm specification, we harvested the culture supernatants of hESCs and their differentiated cells during the mesoderm induction process. Interestingly, a remarkable increase in the levels of PGE_2 in the culture supernatants upon BMP4-induced mesoderm differentiation was observed by enzyme immunoassay (EIA) (Figures 1E and S1F), indicating that PGE_2 might play a role in BMP4 signaling during mesoderm fate determination.

De Novo Synthesis of PGE_2 Is Required for BMP4-Induced Mesoderm Specification of hESCs

To elucidate the role of PGE_2 during the mesoderm differentiation of hESCs, we used a non-selective COX inhibitor, indomethacin, to block the endogenous synthesis of PGE_2 (Figures 2A and S1G). Indomethacin treatment within the concentration range tested showed little impact on the proliferation and survival of BMP4-induced cells (Figures S2A–S2C). Exposure to indomethacin during the mesoderm differentiation process caused significant decreases in the expression of the mesodermal key genes, *BRA*, *MIXL-1*, and *EOMES*, and a striking blockade of the expression of the mesodermal marker BRA at a protein level (Figures 2B–2D and S2D), indicating that endogenous and *de novo* PGE_2 synthesis was required for BMP4-induced mesoderm specification of hESCs. Similarly, mouse epiblast stem cells (EpiSCs), which are derived from pre-gastrula-stage late epiblast, showed little expression of the mesodermal marker genes *Bra* in the absence of endogenous PGE_2 (data not shown). To further investigate the differentiation fate of the indomethacin-treated cells, we grew them in hemato-vascular (HV) progenitor differentiation medium for 4 days (Figure 2A). These indomethacin-treated cells showed differentiation defect in formation of HV precursors. Expression of hematopoietic as well as endothelial marker genes, such as *KDR*, *SCL*, and *VE-CAD*, were all suppressed after indomethacin treatment (Figure 2E). Consistently, the percentage of KDR^+CD31^+ cells was significantly decreased (Figures 2F and 2G). The indomethacin-treated cells presented notably impaired endothelial and cardiac differentiation potential (Figures S2E–S2H), indicating that inhibition of endogenous PGE_2 synthesis led to a mesoderm differentiation block. Furthermore, despite the existing of BMP4 signaling, inhibition of endogenous PGE_2 synthesis by indomethacin significantly raised the level of the early neuroectodermal marker transcripts (*HOXA1*, *ZIC1*, *SOX1*, and *GBX2*), and increased $NESTIN^+PAX6^+$ cell percentage after neural induction (Figures 2H, S2I, and S2J). However, effects of BMP4 on trophectoderm differentiation measured by expression of *GCM1* and *cGA* genes and of cGA protein were not altered by indomethacin (Figures S2K and S2L). All these results indicated that *de novo* synthesis of PGE_2 is required specifically for BMP4-induced mesoderm specification of hESCs, whereas blockade of its synthesis reduced mesoderm specification and enhanced neuroectoderm cell fate commitment of hESCs.

We then performed *ex vivo* transplantation experiments to further evaluate the differentiation potential of these pluripotent cells in the presence of BMP4 induction or absence of PGE_2 synthesis. After 2 days of BMP4 induction in the presence and absence of indomethacin, the differentiated cells were subcutaneously transplanted into NOD/SCID mice. The whole grafts formed from transplanted hESCs treated with BMP4 in the presence of indomethacin demonstrated significantly increased expression of the neuroectodermal markers *NESTIN*, *NEUROD*, *PAX6*, *ZIC1*, and *GFAP* compared with grafts from transplanted

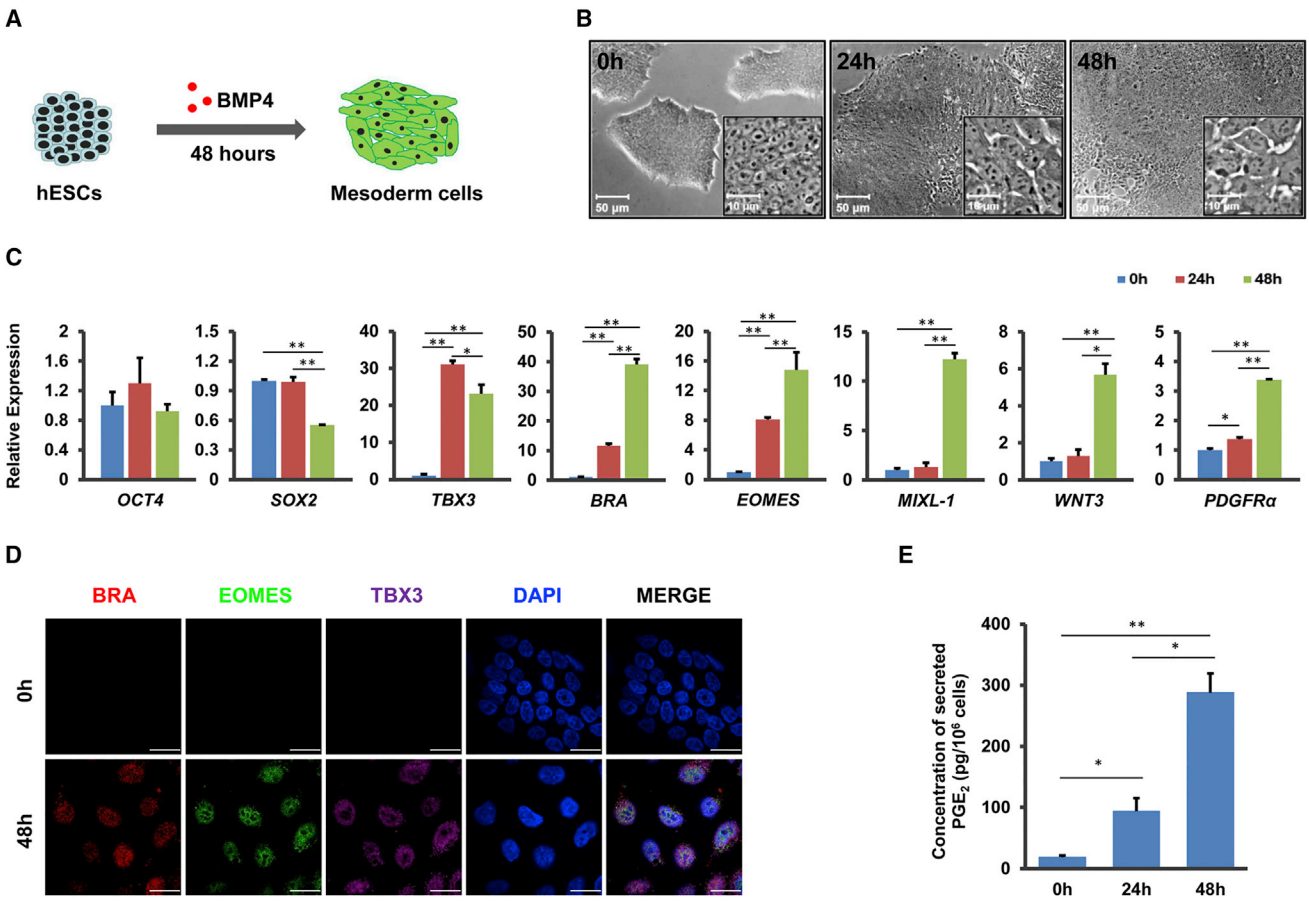

Figure 1. PGE_2 Is Increased upon BMP4-Induced Mesoderm Differentiation

(A) Schematic of mesoderm induction of hESCs.

(B) Morphological changes of BMP4-treated hESCs on different days. Scale bars represent 50 μm (main) and 10 μm (inset).

(C) Lineage-specific gene expression changes in hESCs during mesoderm differentiation (SFDM + 25 ng/mL BMP4, 2 days) were determined by qPCR. *p < 0.05, **p < 0.01 compared with 0 hr. n = 3 independent experiments.

(D) Lineage-specific proteins expression was detected during hESC mesoderm differentiation by immunostaining. Scale bars represent 20 μm.

(E) Secreted PGE_2 levels in the culture medium of hESCs and their differentiated cells were detected by EIA. hESC culture medium was collected as sample at 0 hr. At 24 and 48 hr after BMP4 induction, the culture media were collected for detection of PGE_2 secretion levels (24h and 48h). *p < 0.05, **p < 0.01 compared with 0 hr. n = 3 independent experiments.

Error bars indicate SD. See also Figure S1.

hESCs with BMB4 treatment alone (Figure 2I). In contrast, mesoderm and endoderm lineage marker genes, such as *VE-CAD*, *RUNX1*, *WNT3*, *ACTA2*, *PPARγ*, *SOX9*, and *FOXA2*, were uniformly downregulated in these engrafted tissues (Figure 2I). Consistently, immunostaining of the grafts from hESCs treated with BMP4 in the absence of indomethacin showed more positive staining for mesoderm markers (KDR, ACTA2) and less for neural stem cells and neurons in the intact tissue sections than grafts from hESCs treated with BMP-4 but in the presence of indomethacin (Figures S2M and S2N), indicating that endogenous PGE_2 synthesis is required for BMP4 induction of mesoderm differentiation in hESCs. Blockade of *de novo* PGE_2 synthesis prevented BMP4-induced mesoderm differentiation, whereas it promoted neuroectoderm cell fate of hESCs.

BMP4 Signaling Directly Regulates *COX-1* Gene Expression and Promotes PGE_2 Production

We next investigated how an increase of endogenous PGE_2 level was induced during BMP4-initiated mesoderm differentiation from hESCs. Since PGE_2 was synthesized from arachidonic acid (AA) by two key cyclooxygenases (COX-1 or COX-2), we firstly evaluated the expression of

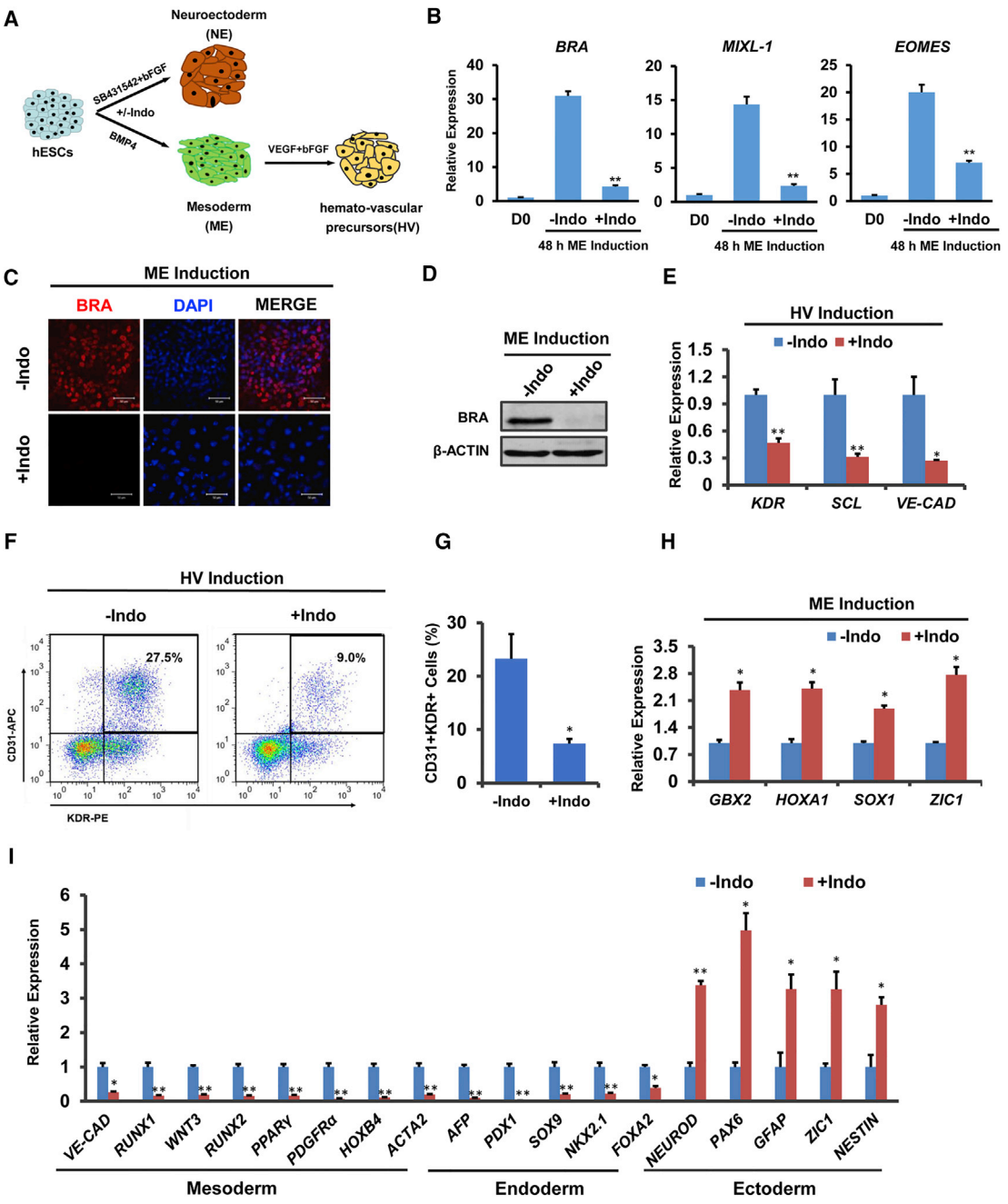

Figure 2. *De Novo* Synthesis of PGE_2 Is Required for BMP4-Induced Mesoderm Specification of hESCs

(A) Schematic of different induction methods. Indo, indomethacin.

(B) qPCR analysis of mesodermal marker gene expression levels in hESCs with BMP4 induction plus DMSO (−Indo) or indomethacin (+Indo) for 48 hr. **$p < 0.01$ compared with −Indo group. $n \geq 3$ independent experiments.

(C and D) Immunostaining (C) and western blotting (D) analysis for BRA in hESCs with BMP4 induction plus DMSO (−Indo) or indomethacin (+Indo) for 48 hr. Scale bars represent 50 μm.

(E) hemato-vascular precursors (HV) marker gene expression levels in hESCs with BMP4 induction plus DMSO (−Indo) or indomethacin (+Indo) for 48 hr and hemato-vascular precursors induction (SFDM + 50 ng/mL VEGF + 50 ng/mL bFGF) for 4 days. *$p < 0.05$, **$p < 0.01$ compared with −Indo group. n = 3 independent experiments.

(F and G) Flow cytometry analysis of the percentage of KDR^+CD31^+ cells after hemato-vascular induction. *$p < 0.05$ compared with −Indo group. n = 3 independent experiments.

(legend continued on next page)

COX-1 and COX-2 in the presence of BMP4. qPCR, western blot, and immunofluorescence analyses revealed that the expression levels of COX-1 mRNA and its protein were notably increased during BMP4-induced mesoderm differentiation in hESCs (Figures 3A–3C). However, the expression of COX-2 mRNA and its protein showed little change during this process (Figures 3A and 3B). Pharmacological inhibition of activation of BMP4 receptor by dorsomorphin resulted in significantly reduced expression of the COX-1 and PGE_2 synthesis in the BMP4-treated hESCs (Figures 3D, S3A, and S3B). Consistently, suppression of SMAD production by siSMAD1 in the downstream of BMP4 also remarkably suppressed the expression of COX-1 and PGE_2 synthesis (Figures 3E, 3F, S3C, and S3D). These results suggested a direct regulation of *COX-1*, a cyclooxygenase for PGE_2 synthesis, by BMP signaling.

To further investigate the transcriptional regulation of *COX-1* by the BMP/SMAD signaling, we cloned the regulatory region of human *COX-1* gene promoter spanning the upstream 1,000 bp to downstream 115 bp around the initiation codon ATG into the pGL3-basic luciferase reporter plasmid. Results from the luciferase activity assay revealed that this reporter containing this region responded well to *SMAD1* overexpression in hESCs (Figure 3G). To further map the location of the SMAD1-responsive element, we made serial truncations in the region and tested their SMAD1 responsiveness. We found that the region between −500 bp and +115 bp of *COX-1* ATG still showed response to *SMAD1* overexpression, whereas no significant activity alteration was observed for the pGL3-basic reporter with the region between −100 and +115 bp sequences (Figure 3G). We also used chromatin immunoprecipitation (ChIP) assays to evaluate the interaction of SMAD1 to the human *COX-1* promoter in hESCs. Four sets of primers were designed to amplify the SMAD1-interacting DNA fragments. The qPCR assay using the second pair of primers showed that BMP4 remarkably induced the recruitment of SMAD1 to the region between −435 bp and −140 bp of the *COX-1* ATG, which contained a putative SMAD-binding element (SBE) (from nucleotides −355 to −359; Figure 3H). To further determine whether the transcriptional activity of *COX-1* promoter is regulated by the putative SBE and SMAD1, we deleted the predicted SBE sequence (CAGAC) in the *COX-1* promoter by PCR and constructed this SBE-less sequence into a pGL3-basic vector, which we named pGL3-Δ(500/+115). Upon comparison of the *COX-1* promoter constructs of pGL3-500/+115 and pGL3-Δ(500/+115), the latter showed significantly impaired luciferase activity in HEK293 cells expressing a high endogenous level of SMAD1 (Figure 3I). However, in SMAD1 silencing cells, SBE deletion did not significantly affect the activity of the *COX-1* promoter (Figure 3I). On the other hand, SMAD1 silencing resulted in a dramatic decrease in the activity of *COX-1* promoter with SBE sequence (Figure 3I), which subsequently inhibited the production of PGE_2 (Figure 3J). These results indicated that COX-1, the key enzyme for PGE_2 production, was directly regulated by BMP signaling through the binding of SMAD1 to the consensus SBE in the COX-1 promoter.

PGE_2 Synthesized by COX-1 Initiates Mesoderm Differentiation of hESCs

To further determine the role of COX-1 and PGE_2 in the early fate decisions of hESCs, we carried out loss-of-function experiments to further study the relationship between the key enzymes of PGE_2 synthesis and hESC differentiation. Notably, selective silencing of *COX-1* expression with two independent small interfering RNAs (siRNAs) or pharmacological blockage of the catalytic function of COX-1 by SC-560 downregulated the mRNA level of mesodermal marker genes, such as *BRA*, *MIXL-1*, and *EOMES* (Figures 4A and 4C). Immunostaining results revealed that the percentage of BRA-positive cells was significantly decreased by *COX-1* knockdown or COX-1 selective inhibitor SC-560 (Figures 4B and 4D). Consistently, the expression of BRA was remarkably blocked by SC-560 (Figure 4E). Both SC-560 and DMH1 (selectively inhibited the BMP-induced Smad1/5/8 activation) were more complete in suppression of mesodermal key marker gene (BRA, MIXL-1, and EOMES) expression (Figure S3E). These inhibitors showed no significant difference on suppression of BRA protein expression (Figure S3F). However, selective silencing of *COX-2* expression or selective inhibition of COX-2 with NS-398 had little effect on the expression of mesodermal genes and their protein (Figures 4C–4E, S3G, and S3H). These results indicated that COX-1 and its products PGE_2 mediated BMP4-induced mesoderm differentiation. Next, we investigated whether overexpression of *COX-1* or exogenous PGE_2 administration promoted mesoderm differentiation in hESCs. Compared with the control group, *COX-1* overexpression significantly drove differentiation of hESCs into mesoderm cells, expressing higher levels of the marker genes *BRA*, *MIXL-1*, and *EOMES* (Figure 4F). Western blot analysis showed that overexpression

(H) Neuroectoderm (NE) marker gene expression levels in hESCs with BMP4 induction plus DMSO (−Indo) or indomethacin (+Indo) for 48 hr. *$p < 0.05$ compared with −Indo group. n = 3 independent experiments.

(I) qPCR analysis of tissue-specific gene expression levels in different engrafts. *$p < 0.05$, **$p < 0.01$ compared with −Indo group. n = 3 independent experiments.

Error bars indicate SD. See also Figure S2.

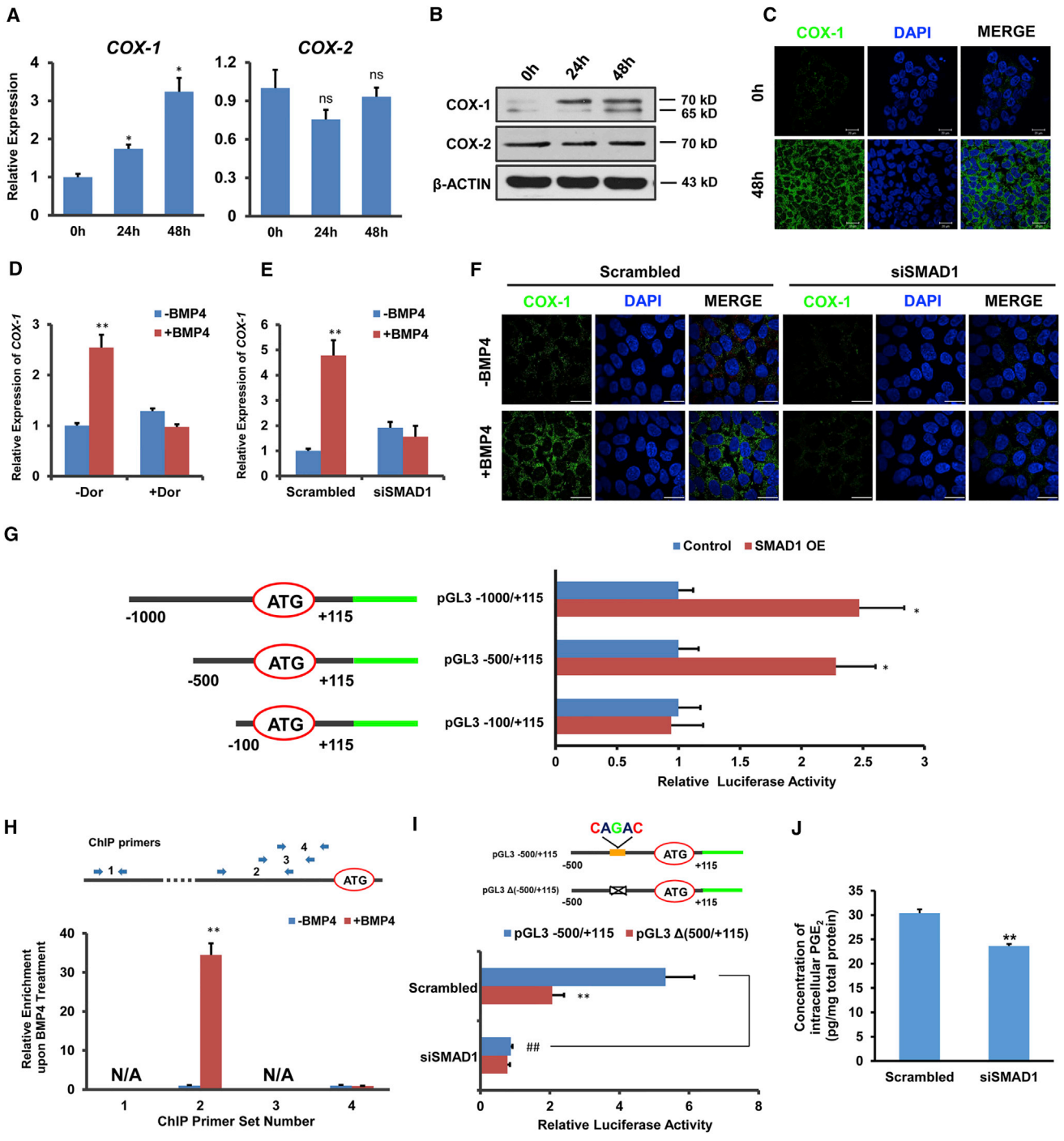

Figure 3. BMP4 Signaling Directly Regulates *COX-1* Gene Expression and Promotes PGE_2 Production

(A) qPCR analysis of *COX-1* and *COX-2* gene expression levels in hESCs after mesoderm induction. *$p < 0.05$ compared with 0 hr. $n \geq 3$ independent experiments.

(B) COX-1 and COX-2 protein expression levels in hESCs after mesoderm induction were determined by western blot analysis.

(C) COX-1 expression was detected during hESC mesoderm differentiation by immunostaining. The nuclei were counterstained with DAPI. Scale bars represent 20 μm.

(D) qPCR analysis of the expression levels of *COX-1* in hESCs treated with vehicle control, BMP4 alone, dorsomorphin (Dor) alone, or BMP4 plus Dor. **$p < 0.01$ compared with −BMP4−Dor group. n = 3 independent experiments.

(legend continued on next page)

of *COX-1* notably enhanced the expression of BRA protein (Figure 4G). We then tested the effect of exogenous PGE_2 on the initiation of early mesoderm differentiation of hESCs. PGE_2 induced expression of *BRA* transcript in a dose-dependent manner in differentiated cells at concentrations between 10 nM and 1 μM (Figure 4H). Similarly, other key mesodermal genes were also markedly upregulated by PGE_2 treatments (Figure 4I). As a control, the differentiated cells from hESCs in the absence of PGE_2 induction exhibited little or undetectable BRA expression. Strong expression of the BRA protein was only detected in PGE_2-treated hESCs (Figures 4J and 4K). Finally, PGE_2 application in mouse EpiSCs also significantly upregulated the expression of mesodermal marker genes and BRA protein (Figures 4L and 4M). These results further suggested that PGE_2 conferred mesoderm fate decision in hESCs and EpiSCs.

PGE_2 Stimulates Mesoderm Differentiation of hESCs through the EP2-PKA-GSK3β/β-Catenin Signaling Pathway

PGE_2 exerts its cellular functions by binding to four G-protein-coupled receptors, which are designated EP1 to EP4. We first detected the expression level of *EP1* to *EP4* in cultured hESCs and found that the expression of *EP2*, *EP3*, and *EP4* was higher than that of *EP1* (Figure S4A). Studies have suggested that EP2 and EP4 are coupled to the stimulation of adenylyl cyclase and result in increased intracellular cyclic AMP (cAMP) production, and EP3 inhibited the formation of cAMP (Sugimoto and Narumiya, 2007). We then investigated whether PGE_2 affected the production of cAMP in hESCs. The results showed that PGE_2 treatment significantly stimulated the formation of cAMP, which suggests that EP2 or EP4 might be activated by PGE_2 (Figure 5A). The expression of these two receptors was significantly detectable in hESCs (Figure 5B). We then added a selective antagonist of EP2 or EP4 to the cultured hESCs before PGE_2 treatment. Application of the EP2 antagonist AH6809 abolished the effects of PGE_2 on the cAMP increase (Figure 5A). In contrast, the EP4 antagonist AH23848 had little effect on the level of cAMP (Figure 5A). Analysis by qPCR revealed that the PGE_2-induced expression of the mesoderm marker genes *BRA* and *MIXL-1* was significantly inhibited by the EP2 antagonist AH6809, but not by the EP4 antagonist AH23848 (Figure 5C). Similarly, EP2 knockdown suppressed the expression of mesoderm marker genes in the presence of PGE_2 (Figure S4B). Consistently, the EP2 agonist butaprost, but not the EP4 agonist PGE_1 alcohol, induced mesodermal marker gene expression (Figure 5D).

We then investigated the downstream signaling pathway associated with PGE_2-EP2 activation. It has been reported that the cAMP-activated protein kinase (PKA) can directly phosphorylate glycogen synthase kinase 3β (GSK-3β) and inhibit its kinase activity (Fang et al., 2000; Fujino et al., 2002; Li et al., 2000). Western blotting results revealed that treatment of hESCs with PGE_2 induced rapid phosphorylation of GSK-3β on Ser9 and β-catenin on Ser675 (Figure 5E). Notably, the EP2 antagonist AH6809 and the PKA inhibitor H89 significantly inhibited the phosphorylation of GSK-3β and β-catenin provoked by PGE_2 (Figure 5F). Conversely, the EP4 antagonist AH23848 did not prevent the activation of GSK-3β or β-catenin. Subsequently, nuclear translocation of β-catenin was observed in response to PGE_2 stimulation (Figure 5G), and its translocation was blocked by the EP2 antagonist or the PKA inhibitor H89 (Figure 5G). These results suggested that PGE_2 induced the mesoderm differentiation of hESCs mainly by activating the EP2-PKA-GSK-3β/β-catenin signaling pathway, which then initiated the expression of its target genes (Figure 6) such as BRA and MIXL-1 (Arnold et al., 2000; Singh et al., 2012).

DISCUSSION

Here, we demonstrated that *de novo* synthesis of PGE_2 was required for BMP4-induced mesoderm specification of hESCs. Our data further showed that one of the key PGE_2

(E and F) qPCR (E) and immunostaining (F) analysis of COX-1 expression levels in siScrambled or siSMAD1-transfected hESCs treated with vehicle control and BMP4. $^{**}p < 0.01$ compared with scrambled-transfected and −BMP4 group. n = 3 independent experiments. Scale bars represent 20 μm.

(G) Effect of SMAD1 on COX-1 transcriptional activity was determined by measuring luciferase activity. Firefly luciferase activity was normalized to control Renilla activity. $^{*}p < 0.05$ compared with control group. n = 3 independent experiments. OE, overexpression.

(H) Binding relationship between SMAD1 and the human COX-1 promoter was determined by ChIP and qPCR assays. $^{**}p < 0.01$ compared with −BMP4 cells. n = 3 independent experiments.

(I) HEK293 cells were transfected with siSMAD1 or Scrambled control and the luciferase activities of pGL3-500/+115 and pGL3 Δ(−500/+115) (Delete CAGAC) were determined. $^{**}p < 0.01$ compared with scrambled+pGL3 −500/+115; $^{\#\#}p < 0.01$ compared with scrambled+pGL3 −500/+115 group. n = 3 independent experiments.

(J) HEK293 cells were transfected with siSMAD1 or Scrambled control and the intracellular PGE_2 concentration was detected by EIA. $^{**}p < 0.01$ compared with scrambled. n = 3 independent experiments.

Error bars indicate SD. See also Figures S3 and S5.

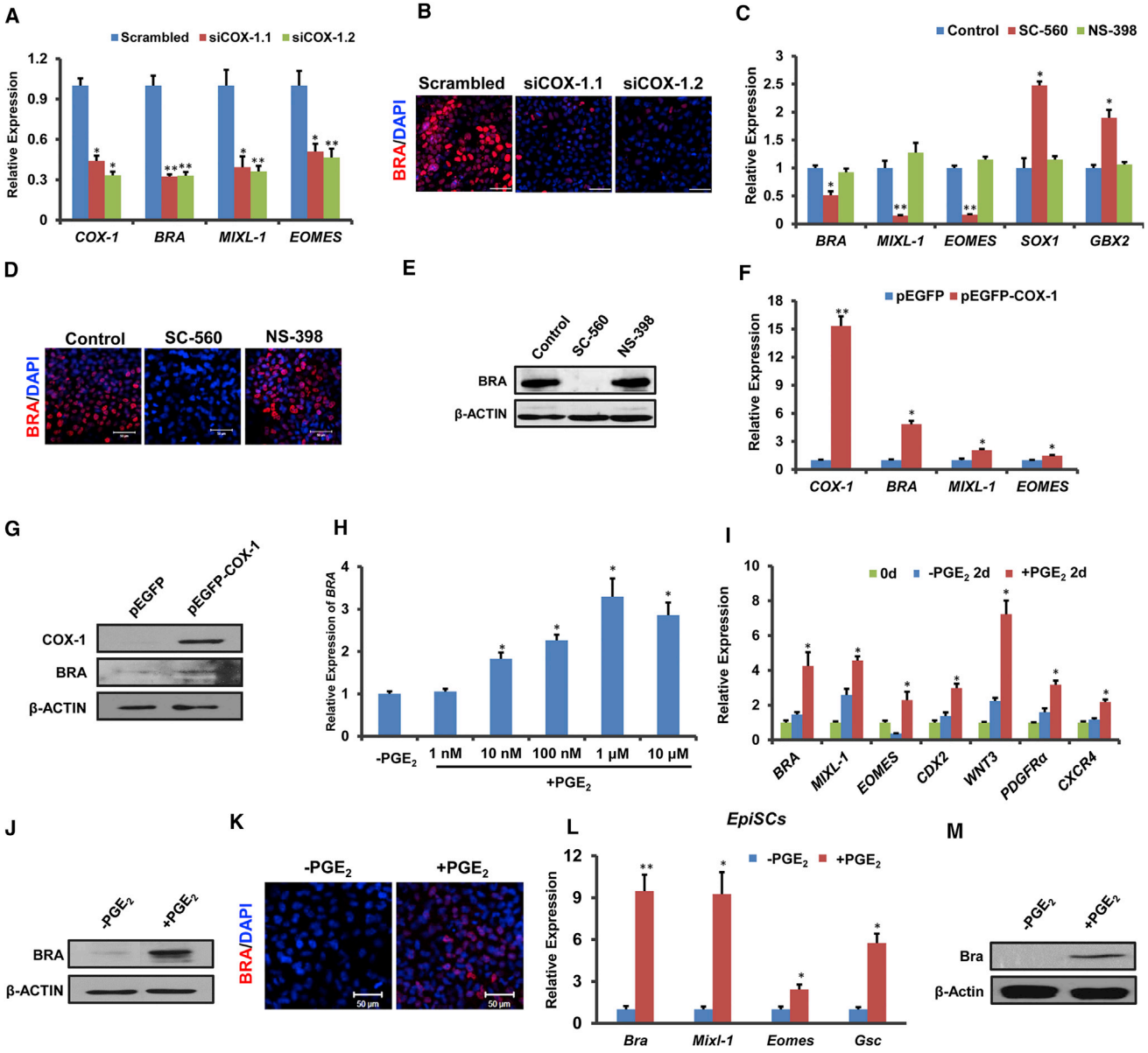

Figure 4. PGE_2 Is Sufficient to Initiate Mesoderm Differentiation of hESCs

(A) qPCR analysis of mesoderm marker gene expression levels in BMP4-induced hESCs transfected with two independent siRNAs against COX-1 or a scrambled control siRNA. *$p < 0.05$, **$p < 0.01$ compared with the scrambled control group. n = 3 independent experiments.

(B) Immunostaining for BRA expression in BMP4-induced hESCs transfected with two independent siRNAs against COX-1 or a scramble control siRNA. Scale bars represent 50 μm.

(C) qPCR analysis of mesoderm marker gene expression levels in hESCs with BMP4 induction plus DMSO (control), SC-560, or NS-398 for 48 hr. *$p < 0.05$, **$p < 0.01$ compared with control group. n = 3 independent experiments.

(D and E) Immunostaining (D) and western blotting (E) analysis for BRA expression in hESCs with BMP4 induction plus DMSO (Control), SC-560, or NS398 for 48 hr. Scale bars represent 50 μm.

(F) Mesoderm gene expression levels in pEGFP-hESCs and pEGFP-COX-1 hESCs during differentiation were determined by qPCR. *$p < 0.05$, **$p < 0.01$ compared with pEGFP-transfected cells. n = 3 independent experiments.

(G) Western blotting analysis for COX-1 and BRA in pEGFP-hESCs and pEGFP-COX-1 transfected hESCs 2 days after transfection.

(H) qPCR analysis of the *BRA* expression levels in hESCs with PGE_2 treatment at different concentration for 2 days. *$p < 0.05$ compared with $-PGE_2$ cells. n = 3 independent experiments.

(legend continued on next page)

synthesis enzymes, COX-1, was crucial for proper differentiation of mesoderm progenitor cells from hESCs, which indicated that COX-1-derived PGE_2 mediated BMP4-induced mesoderm commitment. Our results reveal a previously unknown role for PGE_2 in regulating mesodermal cell fate specification.

It is well known that ESCs are capable of differentiating into three germ layers *in vitro*. However, limiting differentiation of ESCs into a desired cell lineage is still a big challenge. To obtain directed differentiation, it is critical to reveal the complicated signal networks that control ESC fate decisions. It has been reported that BMP4 signaling is required for mesoderm formation and for inhibition of neural induction in mice (Marchal et al., 2009). In hESCs, BMP4 can also promote mesendoderm and mesoderm differentiation, and inhibit neuroectoderm development (Di-Gregorio et al., 2007; Massagué et al., 2005; Tang et al., 1998; Watabe and Miyazono, 2009; Winnier et al., 1995). Despite several signal pathways and some target genes having been reported to participate in BMP4-induced mesoderm specification, the precise regulatory mechanism of BMP4 signaling has remained largely unknown. Recent studies have demonstrated that PGE_2 signaling plays crucial roles in the modulation of angiogenesis, vascular tube formation, and hematopoiesis (Cha et al., 2005; Yang et al., 2010; North et al., 2007). These findings have attracted us to investigate the regulatory role of PGE_2 in the early mesoderm commitment of ESCs. Here, we first tested effect of inhibition of endogenous PGE_2 synthesis, using a PGE_2 synthesis inhibitor indomethacin, on BMP4-induced mesoderm fate decision of hESCs. Surprisingly, indomethacin treatment remarkably suppressed mesoderm progenitor cell commitment and impaired the mesoderm progeny cell differentiation capacity of BMP4-induced cells. Indomethacin at 5–20 μM induced strong blockade of HV differentiation (Figure S5A). We also assessed the endoderm differentiation potential of BMP4-treated cells with or without the presence of indomethacin for 2 days. These two cell populations displayed low definitive endoderm differentiation efficiency (Figure S5B), which might be due to the low expression of endoderm genes (*GSC* and *CXCR4*) as a result of BMP4 treatment (Figure S5C). However, cells in the presence of indomethacin showed significantly decreased expression of endoderm genes (*SOX17* and *GATA4*) compared with that in the absence of indomethacin (Figure S5D). Conversely, indomethacin treatment strongly promoted the neuroectoderm development of hESCs.

PGE_2 is a small-molecule metabolite of AA, synthesized first by COX-1 or COX-2 and then by prostaglandin synthase (Phipps et al., 1991). Increasing evidence has suggested that the requirement of individual COX for PGE_2 production is specific to cell types and functions, especially in early embryonic development (Cha et al., 2005; Goessling et al., 2009; Speirs et al., 2010). COX-1 expression is restricted to the posterior mesoderm during zebrafish somitogenesis (Cha et al., 2005; Grosser et al., 2002). In our study, we found that the expression levels of *COX-1* mRNA and protein were increased during the BMP4-induced differentiation process, which is consistent with the increased levels of PGE_2 in the same process. We then wanted to examine the correlation of BMP4 signal and *COX-1* gene expression. More detailed studies showed that BMP4 recruited SMAD1 to the predicted SBE-containing part of the *COX-1 cis*-regulatory region and directly regulated *COX-1* transcription. Therefore, our results support the hypothesis that *COX-1* acts as a BMP4/SMAD1 downstream target. Another transforming growth factor β superfamily member, Activin A, could not induce either *COX-1* expression or PGE_2 synthesis (Figures S5E and S5F), indicating the specific regulation of *COX*-1 by BMP4. These results further led us to investigate whether COX-1-derived PGE_2 directly regulated early cell fate decisions. We used both COX-1 knockdown and chemical blockade of COX-1 activity approaches to further demonstrate the role of COX-1-derived PGE_2 in mesoderm specification. Selective inhibition of COX-1 activity led to mesoderm differentiation defect in hESCs, revealing the necessity of COX-1-derived PGE_2 for mesoderm differentiation. The critical role of COX-1 in early embryonic development was also proved in the zebrafish model. Knockdown of COX-1 resulted in gastrulation arrest, while COX-2 knockdown failed to produce any phenotype in zebrafish (Speirs et al., 2010). In line with this observation, we found that COX-2 did not participate in BMP4-induced mesoderm differentiation. Importantly, forced *COX-1* expression or PGE_2 treatment was sufficient for the initiation of mesoderm specification of hESCs, demonstrating that PGE_2 signaling positively

(I) qPCR analysis of mesodermal gene expression levels in hESCs treated with 1 μM PGE_2. *$p < 0.05$ compared with $-PGE_2$ 2d. n = 3 independent experiments.

(J and K) Western blotting (J) and immunostaining (K) analysis for BRA in hESCs treated with 1 μM PGE_2 for 2 days. Scale bars represent 50 μm.

(L) qPCR analysis of mesodermal gene expression levels in EpiSCs treated with 1 μM PGE_2. *$p < 0.05$, **$p < 0.01$ compared with $-PGE_2$ 2d. n = 3 independent experiments.

(M) Western blotting analysis for Bra in EpiSCs treated with 1 μM PGE_2 for 2 days.

Error bars indicate SD. See also Figure S3.

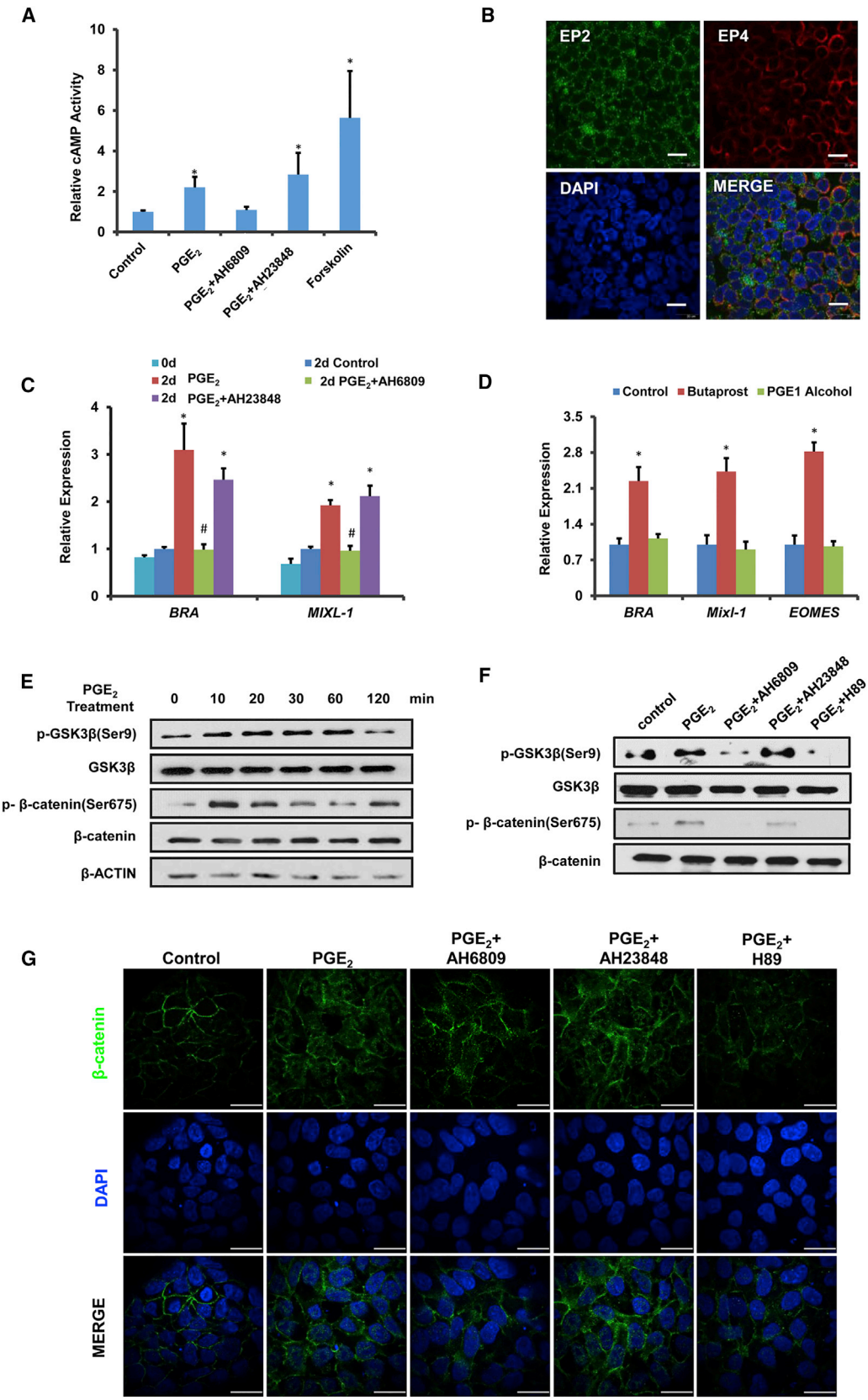

(legend on next page)

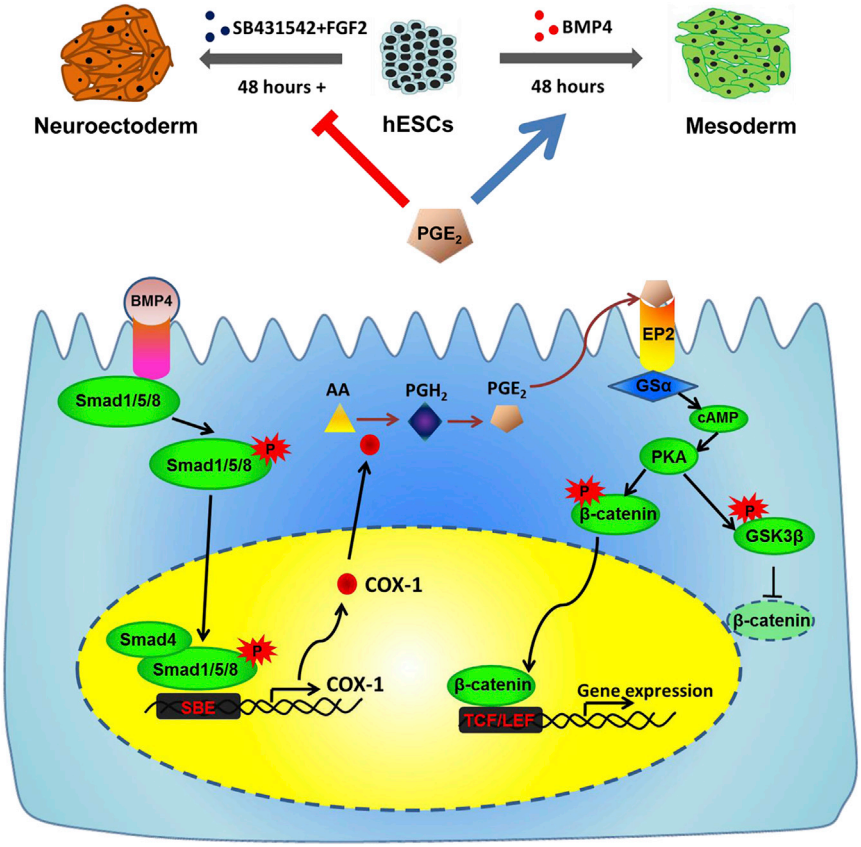

Figure 6. Graphic Representation of the Regulation of COX-1-Derived PGE_2 in the Mesoderm and Neuroectoderm Differentiation of hESCs

regulated mesoderm commitment of hESCs. Furthermore, prolonged exposure to PGE_2 for 7 days caused remarkably increased expression levels of mesoderm marker genes but not neuroectoderm genes (Figure S6A), further supporting the positive role of PGE_2 in mesoderm cell fate commitment.

PGE_2 functions in an either autocrine or paracrine manner via four specific receptors, EP1 to EP4. These receptors, encoded by different genes and expressed specifically in different cells, have complex, sometimes opposite, responses to PGE_2 (Harizi et al., 2003; Panzer and Uguccioni, 2004; Villablanca et al., 2007). PGE_2 can activate different receptors in different cell types, and the interaction of PGE_2 with its receptors can result in activation of different pathways (Castellone et al., 2005; Xia et al., 2010). In our study we found that PGE_2 activated EP2 and PKA signaling, which subsequently induced phosphorylation of GSK-3β (Ser9) and β-catenin (Ser675) in hESCs. Consistently, EP2 agonist notably activated β-catenin in hESCs (Figure S6B). These findings suggest that PKA-GSK-3β/β-catenin is the main downstream effector of PGE_2/EP2 signaling in

Figure 5. PGE_2 Stimulates Mesoderm Differentiation of hESCs through the EP2-PKA-GSK3β/β-Catenin Signaling Pathway

(A) cAMP level of hESCs with vehicle control, Forskolin, PGE_2, PGE_2 + AH6809, or AH23848 treatment were determined by cAMP Glo array. *$p < 0.05$ compared with the control group. n = 3 independent experiments.

(B) EP2 and EP4 receptor expression in hESCs was detected by immunostaining. Scale bars represent 20 μm.

(C) qPCR analysis of the *BRA* and *MIXL-1* expression levels in hESCs treated with vehicle control, PGE_2, PGE_2 + AH6809, or AH23848. *$p < 0.05$ compared with the control group; $^{\#}p < 0.05$ compared with the PGE_2 group. n = 3 independent experiments.

(D) qPCR analysis of the gene expression levels in hESCs treated with vehicle control, butaprost, and PGE_1 alcohol. *$p < 0.05$ compared with the control group. n = 3 independent experiments.

(E) Western blotting analysis for p-GSK3β and p-β-catenin levels in hESCs treated with PGE_2 for different times.

(F) Western blotting analysis for p-GSK3β and p-β-catenin protein expression levels in hESCs treated with vehicle control, PGE_2, PGE_2 + AH6809, PGE_2 + AH23848, or PGE_2 + H89.

(G) Immunostaining analysis for β-catenin protein translocation in hESCs treated with vehicle control, PGE_2, PGE_2 + AH6809, PGE_2 + AH23848, or PGE_2 + H89. Scale bars represent 25 μm.

Error bars indicate SD. See also Figures S4 and S6.

BMP-4-activated hESCs. It has been reported that phosphorylation of β-catenin (Ser675) or GSK-3β (Ser9) stabilizes the β-catenin protein by inhibiting its destruction (Fang et al., 2000; Hino et al., 2005). The activation of Wnt/β-catenin pathway and the accumulation of β-catenin in the nucleus are required for the mesoderm differentiation of ESCs (ten Berge et al., 2008; Tran et al., 2009). We found that CHIR treatment of hESCs markedly induced the expression of key mesoderm genes and their proteins (Figures S6C and S6D). Addition of CHIR rescued the blocking effect of BRA expression caused by indomethacin (Figure S6E). Interestingly, Wnt receptor antagonist Dkk-1 could not block the expression of BRA induced by BMP4, which is consistent with the report by Zhang et al. (2008). However, indomethacin, a PGE_2 synthesis inhibitor, strikingly suppressed mesoderm induction by BMP4. Furthermore, the function of PGE_2 on initiation of mesoderm specification could not be blocked by Wnt secretion inhibitor IWP2 (Figure S6F). These results further suggest that PGE_2 mediates the mesendoderm and early mesoderm-inducing effect of BMP4, which is independent of endogenous WNT3a signaling.

In conclusion, our work presented here elucidates a role for COX-1-derived PGE_2 in mesoderm progenitor cell induction from hESCs and EpiSCs. In particular, our data reveal that mesoderm inducer BMP4 directly upregulated the metabolism enzyme COX-1, providing a mechanism of how BMP4 controls mesoderm differentiation via a metabolism pathway. Our findings also show crosstalk between BMP4 and Wnt/β-catenin signaling via early activation of the PGE_2 pathway. In all, our findings reveal a mechanism for the early cell fate determination of hESCs and provide insights into strategies for mesoderm induction or neuroectoderm specification through increasing or blocking the PGE_2 signaling pathway.

EXPERIMENTAL PROCEDURES

Cell Culture and Differentiation

WA01 and WA09 hESCs (from Wicell Research Institute, hESCs with 40–60 passages were used in all experiments) were cultured on Matrigel (BD Biosciences)-coated wells in mTeSR1 medium (STEMCELL Technologies) according to the manufacturer's protocol. Mouse EpiSCs were grown on fibronectin coated wells in N2B27 medium supplemented with 20 ng/mL Activin A (R&D systems) and 12 ng/mL basic fibroblast growth factor (bFGF) (Millipore). For mesoderm differentiation, hESCs were grown in SFDM consisting of Iscove's modified Dulbecco's medium/F12 (3:1) supplemented with 0.05% lipid-rich BSA, 1 mM Glutamax, 1% non-essential amino acids, 1% insulin-transferrin-selenium (all from Gibco), and 25 ng/mL BMP4 (R&D Systems). For neuroectoderm differentiation, hESCs were grown in SFDM +10 μM SB431542 (Stemgent) + 12 ng/mL bFGF. Other cytokines or small molecules used were the following: vascular endothelial growth factor 165 ($VEGF_{165}$; 50 ng/mL, Peprotech); PGE_2, AH6809 (10 μM), butaprost (5 μM), AH23848 (10 μM), and prostaglandin E_1 alcohol (5 μM) were from Cayman; dorsomorphin (2 μM) was from Stemgent; indomethacin (10 μM), SC-560 (10 μM), and NS-398 (10 μM) were from Sigma-Aldrich; DMH1 (5 μM) was from Selleck. Concentration of inhibitors using in all experiments depend on related references (Liou et al., 2007; North et al., 2007; Rocca et al., 2002; Zhang and Daaka, 2011). All differentiation experiments were repeated at least three times on different passages of hESCs to ensure that the experimental data described were reproducible from one experiment to the next. HEK293 cells were cultured in HDMEM medium with 10% fetal bovine serum (FBS).

qRT-PCR

Total RNA from cultured cells or tissues was extracted using TRIzol reagent (Invitrogen) according to the manufacturer's protocol. One microgram of total RNA was reverse transcribed with the reverse transcriptase M-MLV (Takara) using oligo(dT) primers. qPCR analysis was performed on a Bio-Rad iQ5 system using the SYBR Green PCR Master Mix (TaKaRa). The RNA levels were normalized using GAPDH as an internal control. The data were representative of multiple experiments. The primers are described in detail in Table S1.

siRNA Transfection

siRNAs were purchased from Sigma-Aldrich. The siRNAs (100–200 nM) were transfected into hESCs with Lipofectamine RNAiMAX (Invitrogen) according to the manufacturer's instructions. The knockdown efficiency was determined by analysis of the gene expression levels of the corresponding target molecule. The siRNA information is described in detail in Table S2.

Immunostaining

Cells were washed twice with PBS before being fixed in 4% paraformaldehyde for 20 min at room temperature, permeabilized in PBS with 0.2% Triton X-100 for 10 min, and blocked in PBS with 10% normal donkey serum for 30 min at room temperature. The cells were then incubated with diluted primary antibody in PBS with 10% donkey serum at 4°C overnight followed by incubation with the corresponding secondary antibody in the dark at room temperature for 40 min. The cells were washed with PBS three times between each step. The nuclei were counterstained with 4′,6-diamidino-2-phenylindole (DAPI) before visualization and image acquisition under a microscope. The antibodies used were as follows: COX-1 (ab109025) and COX-2 (ab15191) were from Abcam; BRA (AF2085) was from R&D Systems; EP2 (sc-20675) and EP4 (sc-55596) were from Santa Cruz Biotechnology.

Flow Cytometry

The cells were trypsinized into single-cell suspensions using 0.25% trypsin (Gibco) and resuspended in PBS containing 5% FBS. The cells were washed and incubated with isotypic antibodies or the indicated antibodies in the dark for 45 min at 4°C. After incubation, the cells were washed three times with PBS and suspended in 0.4 mL of PBS for analysis. 7-Aminoactinomycin D (BD Biosciences) was added to each sample and incubated for 5 min before analysis to eliminate the dead cells. Flow-cytometry analysis

was performed using FACSCalibur (BD Biosciences). The antibodies used were as follows: KDR-PE (560494) was from BD Bioscience; CD31-APC (17-0319-42) was from eBioscience.

Western Blotting

The cells were lysed with RIPA buffer. The homogenates were centrifuged, and the supernatants collected and stored at −80°C. The protein concentrations were determined with the BCA protein assay (Pierce). Equal amounts of proteins were separated using 10%–12% SDS-PAGE and transferred to PVDF membranes. The membranes were blocked with 5% skimmed milk for 1 hr at room temperature and blotted with the primary antibody overnight at 4°C followed by horseradish peroxidase-coupled secondary antibodies. The antigens were revealed using ECL reagents (Millipore). The antibodies used were as follows: β-catenin (Ser675) Antibody Duet (11887), GSK-3β (9315), and pGSK-3β (Ser9) (9322) were from Cell Signaling; COX-1 (ab109025) and COX-2 (ab15191) were from Abcam; BRA (AF2085) was from R&D Systems.

Luciferase Assays

SMAD1 overexpression plasmid (Addgene) and pGL3-basic plasmids containing different fragments of COX-1 promoter were co-transfected into hESCs with Neon Transfection System (Invitrogen). The pRL-CMV plasmid was co-transfected for normalization. The cells were harvested 48 hr later for luciferase assay. Luciferase activity was measured using the dual luciferase assay kit (Promega). All assays were performed in triplicate, and all values were normalized by Renilla luciferase activity.

Chromatin Immunoprecipitation Assays

hESCs were treated with 25 ng/mL BMP4 for 120 min followed by the ChIP assays. The detailed methods are described in Zhang et al. (2012). Four micrograms of the SMAD1 antibody (Santa Cruz, sc-7965) was used for immunoprecipitation, and normal mouse immunoglobulin G was used as a negative control. The DNA was precipitated and purified by the Wizard SV Gel and PCR Clean Up system (Promega), and was used as a template for qPCR to amplify the proximal promoter of COX-1. The primers are described in detail in Table S3.

cAMP Luminescence Assay

Samples containing 1×10^4 cells were exposed to different treatments for 15 min. The luminescence assay was performed according to the standard protocol of the manufacturer (Promega, cAMP Glow).

PGE_2 EIA Assay

The culture supernatants of hESCs and the differentiated cells were collected and dead cells were eliminated by centrifugation. The secreted PGE_2 concentrations were determined by EIA kits according to the manufacturer's protocol (Enzo).

Statistical Analyses

The data are presented as mean ± SD. Student's t test was used for the statistical analysis between two groups. One-way ANOVA was used to compare means among three or more independent groups. $p < 0.05$ was considered significant.

SUPPLEMENTAL INFORMATION

Supplemental Information includes Supplemental Experimental Procedures, six figures, and three tables and can be found with this article online at https://doi.org/10.1016/j.stemcr.2018.01.024.

AUTHOR CONTRIBUTIONS

Y.H.L. and X.T.P. conceived and designed the experiments; B.W.Z., L.J.H., Y.M.L., J.Z., Q.Z., S.H.W., Z.F., F.F., L.C., and Y.L. performed the experiments; J.F.X., B.W.Z., W.Y., and Y.H.L. analyzed the data; B.W.Z. and Y.H.L. wrote the paper; B.W.Z. and L.J.H. contributed equally to this article.

ACKNOWLEDGMENTS

We thank Qiang Wang and Yi Zhou for helpful discussion and specially thank to Yi Zhou for his assistance in editing of the manuscript. We are grateful to Thomas E. Eling for his generous gift of pGL3-COX-1 promoter plasmid. We are grateful to Qi Zhou for his generous gift of mEpiSCs. We thank Tissue Gnostics for FACS-like tissue cytometry analysis. This work was supported by The National Key Research and Development Program of China (nos. 2017YFA0103100, 2017YFA0103103, 2017YFA0103104), the National Natural Science Foundation of China (nos. 31101040, 81472908), Guangdong Frontier and Key Technology Innovation Project (no. 2014B020228001), Guangdong Major Scientific and Technological Project (no. 2013A022100005), and Guangzhou Health Care and Cooperative Innovation Major Project (nos. 201508020257, 201508020262, 201704020218).

Received: March 29, 2017
Revised: January 20, 2018
Accepted: January 22, 2018
Published: February 22, 2018

REFERENCES

Arnold, S.J., Stappert, J., Bauer, A., Kispert, A., Herrmann, B.G., and Kemler, R. (2000). Brachyury is a target gene of the Wnt/beta-catenin signaling pathway. Mech. Dev. *91*, 249–258.

Beppu, H., Kawabata, M., Hamamoto, T., Chytil, A., Minowa, O., Noda, T., and Miyazono, K. (2000). BMP type II receptor is required for gastrulation and early development of mouse embryos. Dev. Biol. *221*, 249–258.

Castellone, M.D., Teramoto, H., Williams, B.O., Druey, K.M., and Gutkind, J.S. (2005). Prostaglandin E_2 promotes colon cancer cell growth through a Gs-axin-beta-catenin signaling axis. Science *310*, 1504–1510.

Cha, Y.I., Kim, S.H., Solnica-Krezel, L., and Dubois, R.N. (2005). Cyclooxygenase-1 signaling is required for vascular tube formation during development. Dev. Biol. *282*, 274–283.

Chng, Z., Teo, A., Pedersen, R.A., and Vallier, L. (2010). SIP1 mediates cell-fate decisions between neuroectoderm and mesendoderm in human pluripotent stem cells. Cell Stem Cell *6*, 59–70.

Di-Gregorio, A., Sancho, M., Stuckey, D.W., Crompton, L.A., Godwin, J., Mishina, Y., and Rodriguez, T.A. (2007). BMP signalling inhibits premature neural differentiation in the mouse embryo. Development *134*, 3359–3369.

Drukker, M., Tang, C., Ardehali, R., Rinkevich, Y., Seita, J., Lee, A.S., Mosley, A.R., Weissman, I.L., and Soen, Y. (2012). Isolation of primitive endoderm, mesoderm, vascular endothelial and trophoblast progenitors from human pluripotent stem cells. Nat. Biotechnol. *30*, 531–542.

Fang, X., Yu, S.X., Lu, Y., Bast, R.C., Jr., Woodgett, J.R., and Mills, G.B. (2000). Phosphorylation and inactivation of glycogen synthase kinase 3 by protein kinase A. Proc. Natl. Acad. Sci. USA *97*, 11960–11965.

Fujino, H., West, K.A., and Regan, J.W. (2002). Phosphorylation of glycogen synthase kinase-3 and stimulation of T-cell factor signaling following activation of EP2 and EP4 prostanoid receptors by prostaglandin E_2. J. Biol. Chem. *277*, 2614–2619.

Goessling, W., North, T.E., Loewer, S., Lord, A.M., Lee, S., Stoick-Cooper, C.L., Weidinger, G., Puder, M., Daley, G.Q., Moon, R.T., et al. (2009). Genetic interaction of PGE_2 and Wnt signaling regulates developmental specification of stem cells and regeneration. Cell *136*, 1136–1147.

Grosser, T., Yusuff, S., Cheskis, E., Pack, M.A., and FitzGerald, G.A. (2002). Developmental expression of functional cyclooxygenases in zebrafish. Proc. Natl. Acad. Sci. USA *99*, 8418–8423.

Harizi, H., Grosset, C., and Gualde, N. (2003). Prostaglandin E_2 modulates dendritic cell function via EP2 and EP4 receptor subtypes. J. Leukoc. Biol. *73*, 756–763.

Hino, S., Tanji, C., Nakayama, K.I., and Kikuchi, A. (2005). Phosphorylation of beta-catenin by cyclic AMP-dependent protein kinase stabilizes beta-catenin through inhibition of its ubiquitination. Mol. Cell. Biol. *25*, 9063–9072.

Hoggatt, J., Singh, P., Sampath, J., and Pelus, L.M. (2009). Prostaglandin E_2 enhances hematopoietic stem cell homing, survival, and proliferation. Blood *113*, 5444–5455.

Kurek, D., Neagu, A., Tastemel, M., Tüysüz, N., Lehmann, J., van de Werken, H.J., Philipsen, S., van der Linden, R., Maas, A., van IJcken, W.F., et al. (2015). Endogenous WNT signals mediate BMP-induced and spontaneous differentiation of epiblast stem cells and human embryonic stem cells. Stem Cell Reports *4*, 114–128.

Leahy, K.M., Koki, A.T., and Masferrer, J.L. (2000). Role of cyclooxygenases in angiogenesis. Curr. Med. Chem. *7*, 1163–1170.

Li, M., Wang, X., Meintzer, M.K., Laessig, T., Birnbaum, M.J., and Heidenreich, K.A. (2000). Cyclic AMP promotes neuronal survival by phosphorylation of glycogen synthase kinase 3beta. Mol. Cell. Biol. *20*, 9356–9363.

Liou, J.Y., Ellent, D.P., Lee, S., Goldsby, J., Ko, B.S., Matijevic, N., Huang, J.C., and Wu, K.K. (2007). Cyclooxygenase-2-derived prostaglandin E2 protects mouse embryonic stem cells from apoptosis. Stem Cells *25*, 1096–1103.

Marchal, L., Luxardi, G., Thomé, V., and Kodjabachian, L. (2009). BMP inhibition initiates neural induction via FGF signaling and Zic genes. Proc. Natl. Acad. Sci. USA *106*, 17437–17442.

Massagué, J., Seoane, J., and Wotton, D. (2005). Smad transcription factors. Genes Dev. *19*, 2783–2810.

Matulka, K., Lin, H.H., Hříbková, H., Uwanogho, D., Dvořák, P., and Sun, Y.M. (2013). PTP1B is an effector of activin signaling and regulates neural specification of embryonic stem cells. Cell Stem Cell *13*, 706–719.

Mishina, Y., Suzuki, A., Ueno, N., and Behringer, R.R. (1995). Bmpr encodes a type I bone morphogenetic protein receptor that is essential for gastrulation during mouse embryogenesis. Genes Dev. *9*, 3027–3037.

Murry, C.E., and Keller, G. (2008). Differentiation of embryonic stem cells to clinically relevant populations: lessons from embryonic development. Cell *132*, 661–680.

Ng, E.S., Azzola, L., Sourris, K., Robb, L., Stanley, E.G., and Elefanty, A.G. (2005). The primitive streak gene Mixl1 is required for efficient haematopoiesis and BMP4-induced ventral mesoderm patterning in differentiating ES cells. Development *132*, 873–884.

North, T.E., Goessling, W., Walkley, C.R., Lengerke, C., Kopani, K.R., Lord, A.M., Weber, G.J., Bowman, T.V., Jang, I.H., Grosser, T., et al. (2007). Prostaglandin E_2 regulates vertebrate haematopoietic stem cell homeostasis. Nature *447*, 1007–1011.

Panzer, U., and Uguccioni, M. (2004). Prostaglandin E_2 modulates the functional responsiveness of human monocytes to chemokines. Eur. J. Immunol. *34*, 3682–3689.

Phipps, R.P., Stein, S.H., and Roper, R.L. (1991). A new view of prostaglandin E regulation of the immune response. Immunol. Today *12*, 349–352.

Rocca, B., Secchiero, P., Ciabattoni, G., Ranelletti, F.O., Catani, L., Guidotti, L., Melloni, E., Maggiano, N., Zauli, G., and Patrono, C. (2002). Cyclooxygenase-2 expression is induced during human megakaryopoiesis and characterizes newly formed platelets. Proc. Natl. Acad. Sci. USA *99*, 7634–7639.

Ruan, Y.C., Guo, J.H., Liu, X., Zhang, R., Tsang, L.L., Dong, J.D., Chen, H., Yu, M.K., Jiang, X., Zhang, X.H., et al. (2012). Activation of the epithelial Na^+ channel triggers prostaglandin E(2) release and production required for embryo implantation. Nat. Med. *18*, 1112–1117.

Singh, A.M., Reynolds, D., Cliff, T., Ohtsuka, S., Mattheyses, A.L., Sun, Y., Menendez, L., Kulik, M., and Dalton, S. (2012). Signaling network crosstalk in human pluripotent cells: a Smad2/3-regulated switch that controls the balance between self-renewal and differentiation. Cell Stem Cell *10*, 312–326.

Speirs, C.K., Jernigan, K.K., Kim, S.H., Cha, Y.I., Lin, F., Sepich, D.S., DuBois, R.N., Lee, E., and Solnica-Krezel, L. (2010). Prostaglandin $G\beta\gamma$ signaling stimulates gastrulation movements by limiting cell adhesion through Snai1a stabilization. Development *137*, 1327–1337.

Sugimoto, Y., and Narumiya, S. (2007). Prostaglandin E receptors. J. Biol. Chem. *282*, 11613–11617.

Tang, S.J., Hoodless, P.A., Lu, Z., Breitman, M.L., McInnes, R.R., Wrana, J.L., and Buchwald, M. (1998). The Tlx-2 homeobox gene is a downstream target of BMP signalling and is required for mouse mesoderm development. Development *125*, 1877–1887.

ten Berge, D., Koole, W., Fuerer, C., Fish, M., Eroglu, E., and Nusse, R. (2008). Wnt signaling mediates self-organization and axis formation in embryoid bodies. Cell Stem Cell *3*, 508–518.

Thomson, J.A., Itskovitz-Eldor, J., Shapiro, S.S., Waknitz, M.A., Swiergiel, J.J., Marshall, V.S., and Jones, J.M. (1998). Embryonic stem cell lines derived from human blastocysts. Science *282*, 1145–1147.

Tran, T.H., Wang, X., Browne, C., Zhang, Y., Schinke, M., Izumo, S., and Burcin, M. (2009). Wnt3a-induced mesoderm formation and cardiomyogenesis in human embryonic stem cells. Stem Cells *27*, 1869–1878.

Vallier, L., Touboul, T., Chng, Z., Brimpari, M., Hannan, N., Millan, E., Smithers, L.E., Trotter, M., Rugg-Gunn, P., Weber, A., et al. (2009). Early cell fate decisions of human embryonic stem cells and mouse epiblast stem cells are controlled by the same signalling pathways. PLoS One *4*, e6082.

Villablanca, E.J., Pistocchi, A., Court, F.A., Cotelli, F., Bordignon, C., Allende, M.L., Traversari, C., and Russo, V. (2007). Abrogation of prostaglandin E_2/EP4 signaling impairs the development of $rag1^+$ lymphoid precursors in the thymus of zebrafish embryos. J. Immunol. *179*, 357–364.

Wang, Z., Oron, E., Nelson, B., Razis, S., and Ivanova, N. (2012). Distinct lineage specification roles for NANOG, OCT4, and SOX2 in human embryonic stem cells. Cell Stem Cell *10*, 440–454.

Watabe, T., and Miyazono, K. (2009). Roles of TGF-beta family signaling in stem cell renewal and differentiation. Cell Res. *19*, 103–115.

Wiles, M.V., and Johansson, B.M. (1997). Analysis of factors controlling primary germ layer formation and early hematopoiesis using embryonic stem cell in vitro differentiation. Leukemia *11* (*Suppl 3*), 454–456.

Winnier, G., Blessing, M., Labosky, P.A., and Hogan, B.L. (1995). Bone morphogenetic protein-4 is required for mesoderm formation and patterning in the mouse. Genes Dev. *9*, 2105–2116.

Xia, X., Batra, N., Shi, Q., Bonewald, L.F., Sprague, E., and Jiang, J.X. (2010). Prostaglandin promotion of osteocyte gap junction function through transcriptional regulation of connexin 43 by glycogen synthase kinase 3/beta-catenin signaling. Mol. Cell. Biol. *30*, 206–219.

Yang, C., Xi, J.-F., Xie, X.-Y., Yue, W., Wang, R.-Y., Wu, Q., He, L.-J., Nan, X., Li, Y.-H., and Pei, X.-T. (2010). Prostaglandin E_2 promotes hematopoietic development from human embryonic stem cells. Front. Biol. *5*, 445–454.

Zhang, J., Wang, S., Yuan, L., Yang, Y., Zhang, B., Liu, Q., Chen, L., Yue, W., Li, Y., and Pei, X. (2012). Neuron-restrictive silencer factor (NRSF) represses cocaine- and amphetamine-regulated transcript (CART) transcription and antagonizes cAMP-response element-binding protein signaling through a dual NRSE mechanism. J. Biol. Chem. *287*, 42574–42587.

Zhang, P., Li, J., Tan, Z., Wang, C., Liu, T., Chen, L., Yong, J., Jiang, W., Sun, X., Du, L., et al. (2008). Short-term BMP-4 treatment initiates mesoderm induction in human embryonic stem cells. Blood *111*, 1933–1941.

Zhang, Y., and Daaka, Y. (2011). PGE_2 promotes angiogenesis through EP4 and PKA Cgamma pathway. Blood *118*, 5355–5364.